

1

2 **Supplementary Information for**

3 **Mechanical adaptation of monocytes** in model lung capillary networks

4 Jules Dupire, Pierre-Henri Puech, Emmanuèle Helfer and Annie Viallat

5 Corresponding to Annie Viallat.

6 E-mail: annie.viallat@univ-amu.fr

7 **This PDF file includes:**

8 Supplementary text

9 Figs. S1 to S7

10 Captions for Movies S1 to S7

11 **Other supplementary materials for this manuscript include the following:**

12 Movies S1 to S7

13 Supporting Information Text

14 **Methods. Fabrication of the channel network.** The microfluidic device is made of polydimethylsiloxane (PDMS) (Sylgard
15 184, Dow Corning). PDMS is mixed with the curing agent in a 10:1 ratio and poured on a silicon master pre-treated with silane
16 (tridecafluoro-1,1,2,2-tetrahydrooctyl-trichlorosilane, ABCR) to help the release of the numerous pillars to form a 3-4 mm thick
17 layer. It is degazed, then cross-linked for 2 h at 65°C. Once polymerized, the PDMS chip is carefully peeled off the master and
18 its inlet and outlet are drilled open with a 0.75-mm diameter punch. The microfluidic device is finally assembled by bounding
19 the chip to a PDMS-coated coverslip after O₂ plasma treatment. The silicon master presenting the channel designs in positive
20 relief was fabricated in the clean room facility PLANETE (CT-PACA Micro- and Nanofabrication Platform, Marseille, France)
21 by performing optical soft lithography on a coating of 7 micrometers of SU8 resist (MicroChem) on a silicon wafer, pre-cleaned
22 with piranha and Argon/O₂ plasma. The channel design was done with Clewin software (Clewin Layout Software, Wieweb
23 Inc.) on a chromium mask, which was fabricated by FEMTO-ST (Besançon).

24 **Microfluidic experiment.** The chip inlet and outlet are connected via Teflon tubing (0.013" inner diameter (ID) and
25 0.027" outer diameter (OD) for the inlet, 0.015" ID and 0.027" OD for the outlet) to a flow controller system (MFCS-8C,
26 Fluigent) that allows controlling the pressure drop between inlet and outlet and the circulation of cell suspensions in the
27 microfluidic network. The device is placed on an inverted microscope (IX71, Olympus) equipped with high-speed cameras
28 (Photon-Focus and Photron) and objectives (x20, x40, x60), in an isolated chamber for temperature control. Cells are observed
29 in brightfield. The experiments are done at 37°C.

30 **Image acquisition and analysis.** Movies of cells transiting in the channels are acquired at various frame rate, from 25
31 to 1000 fps, depending on the applied pressure drop. Matlab custom routine was written for automating the image analysis
32 steps. Cell contour with sub-pixel precision is obtained after a combination of background subtraction, intensity thresholding
33 and morphological optimization. It allows a good approximation of the cell volume, surface, sphere diameter and reduced
34 volume, and center of mass position. To increase the precision of the values, we corrected the barrel distortion induced by
35 the objectives. We measured the apparent surface of the pillars of the network, and fit the 2D data with a 2D parabol. This
36 provided 2D maps of the corrective factor for the perimeter and the projected area.

37 **Micropipette experiment and analysis.** Micropipettes of 5 and 7.5 μm in diameter were made from glass capillaries as
38 previously described in Freppel et al. (Sci. Rep. 6:3365 (2016)). Prior to experiment the micropipette inner walls are passivated
39 with a PBS solution supplemented with 1% BSA. The micropipette is mounted on an xyz micromanipulator (Narishige) and
40 inserted in a home-made observation chamber first filled with PBS/1%BSA for outer wall passivation then with complete
41 cell medium. Aspiration of cells (typically 15 μm in diameter) is performed using a homemade aspiration system based on
42 interconnected reservoirs and the aspiration pressure is monitored using pressure sensors. The system is installed on an inverted
43 microscope (IMT2, Olympus) equipped with a camera (GE680, Prosilica) and a 40x objective. Experiments are performed
44 at 23°C. Movies of cell aspiration into micropipette are analyzed using ImageJ software to measure when the cell enters the
45 pipette and then the length pulled in the pipette as function of the pressure difference.

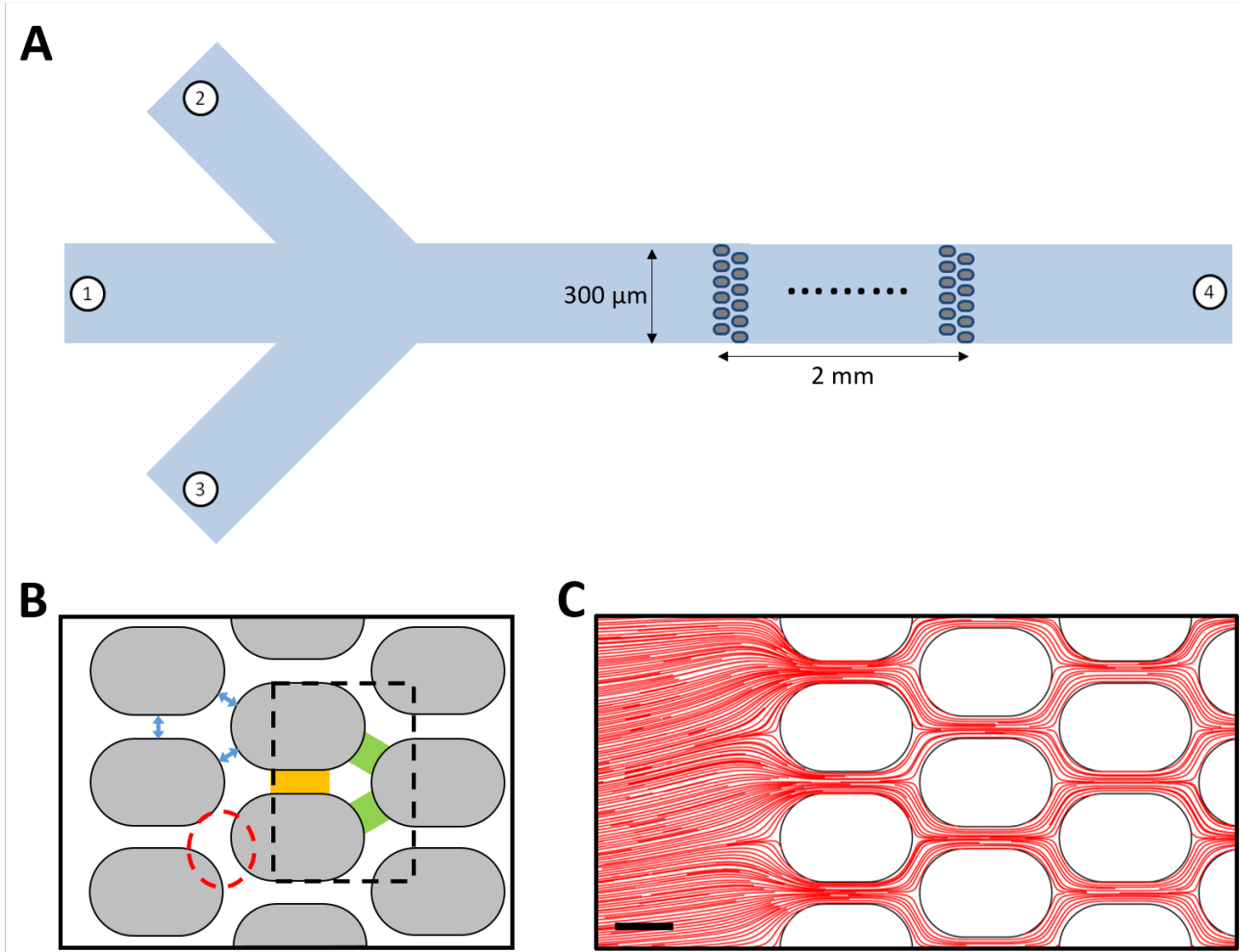


Fig. S1. The microchannel network and its geometrical parameters. A) Schematics of the microfluidic chip, with inlets 1-3 and outlet 4 connected to the flow controller, and the channel network in the middle of the 300- μm wide main channel. The height is equal to 9.3 μm along the whole chip. The total length and width of a network are approximately 300 μm and 2 mm in length, respectively. B) Microchannels are defined by equally spaced pillars (blue arrows). Horizontal and diagonal channels are highlighted in orange and green, respectively. The dashed rectangle corresponds to the network unit mesh, typically 35 x 50 μm^2 , consisting of a horizontal channel, a bifurcation and the two diagonal channels after the bifurcation. The dashed red circle highlights the region combining a bifurcation followed by a diagonal channel (named *diag* position in the main text). C) Comsol 2D-simulation of the streamlines in the network. Scale bar: 15 μm .

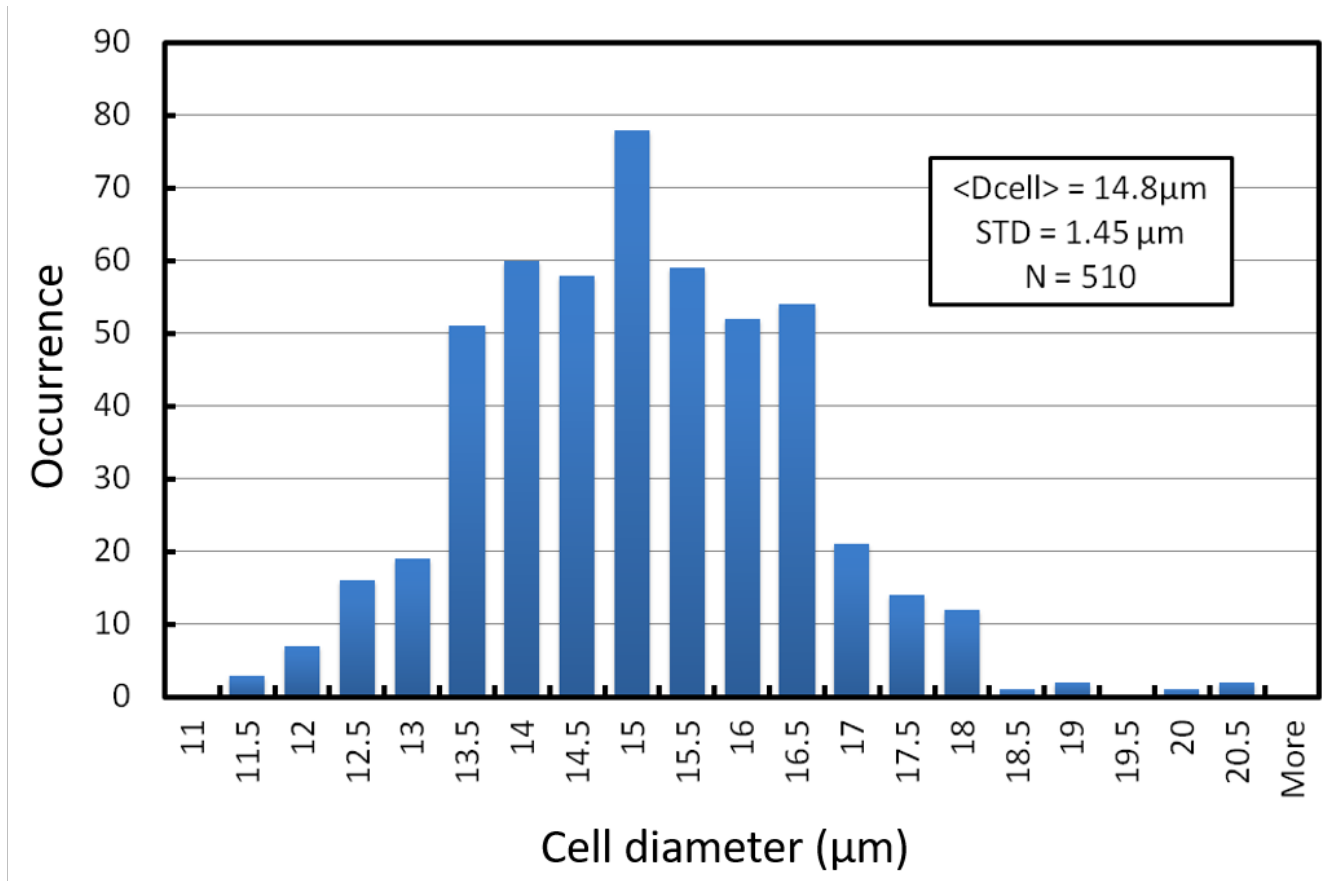


Fig. S2. THP1-cells size distribution

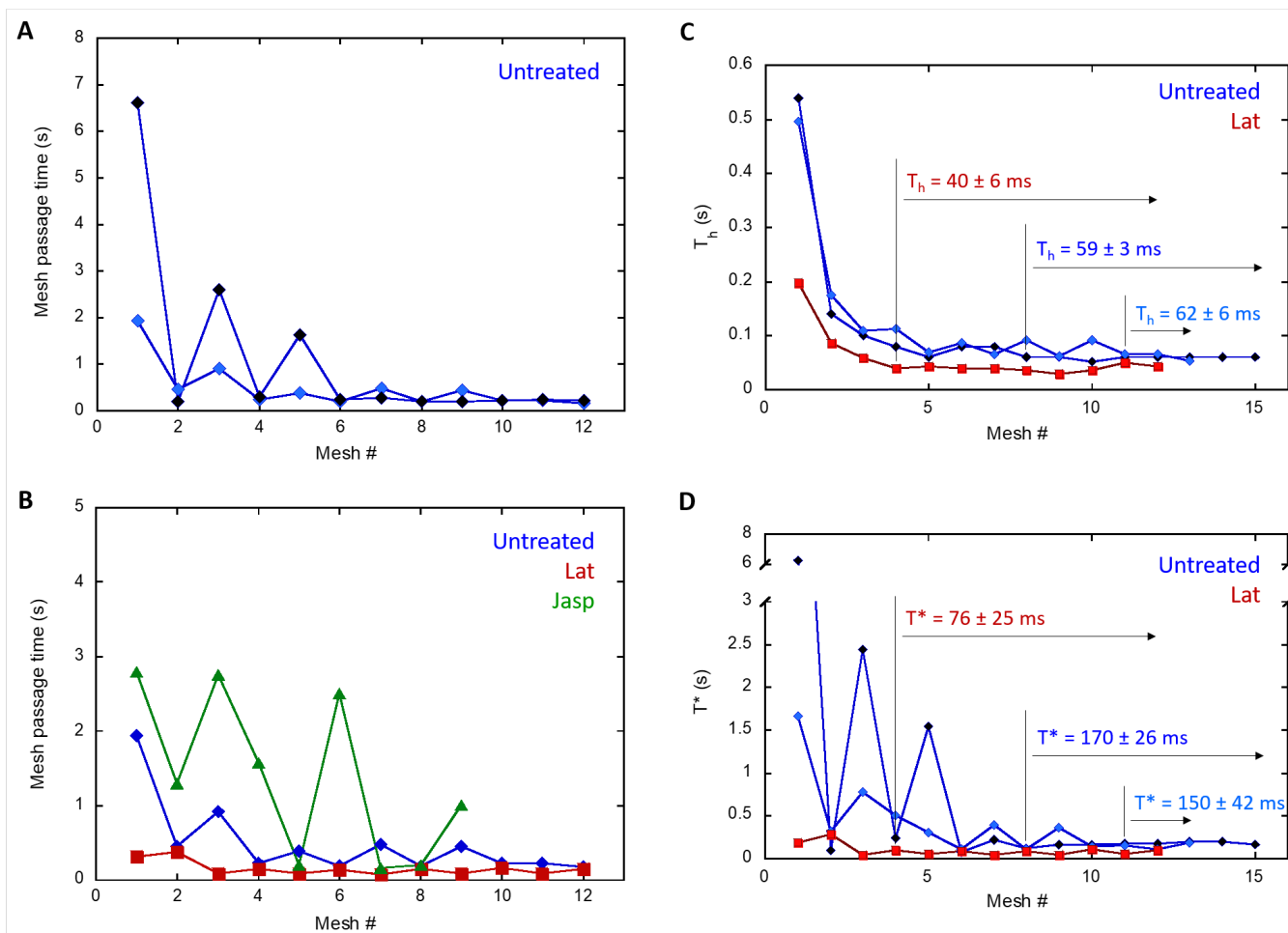


Fig. S3. Cell transit times through the microchannels. A-B) Mesh global passage time, defined as the time a cell takes to move from its position in the middle of a horizontal channel to the same position in the next channel. A) Two untreated cells of $16 \mu\text{m}$ in diameter from the entry in the network (mesh 1) till mesh 12. Cells first alternate between slow and fast transit till they reach the steady-state regime (at different positions in the network), in which they pass through the meshes within 0.2 sec. B) Comparison between untreated, lat-, and jasp-cells of similar size (diameter $\approx 17 \mu\text{m}$) in an $8.6\text{-}\mu\text{m}$ channel network, $\Delta P = 20$ mbar. C-D) Transit times through horizontal channel T_h and *diag* position T^* for the untreated cells from (A) and the lat-cell from (B). The mean values are calculated once the cells have reached the steady-state regime.

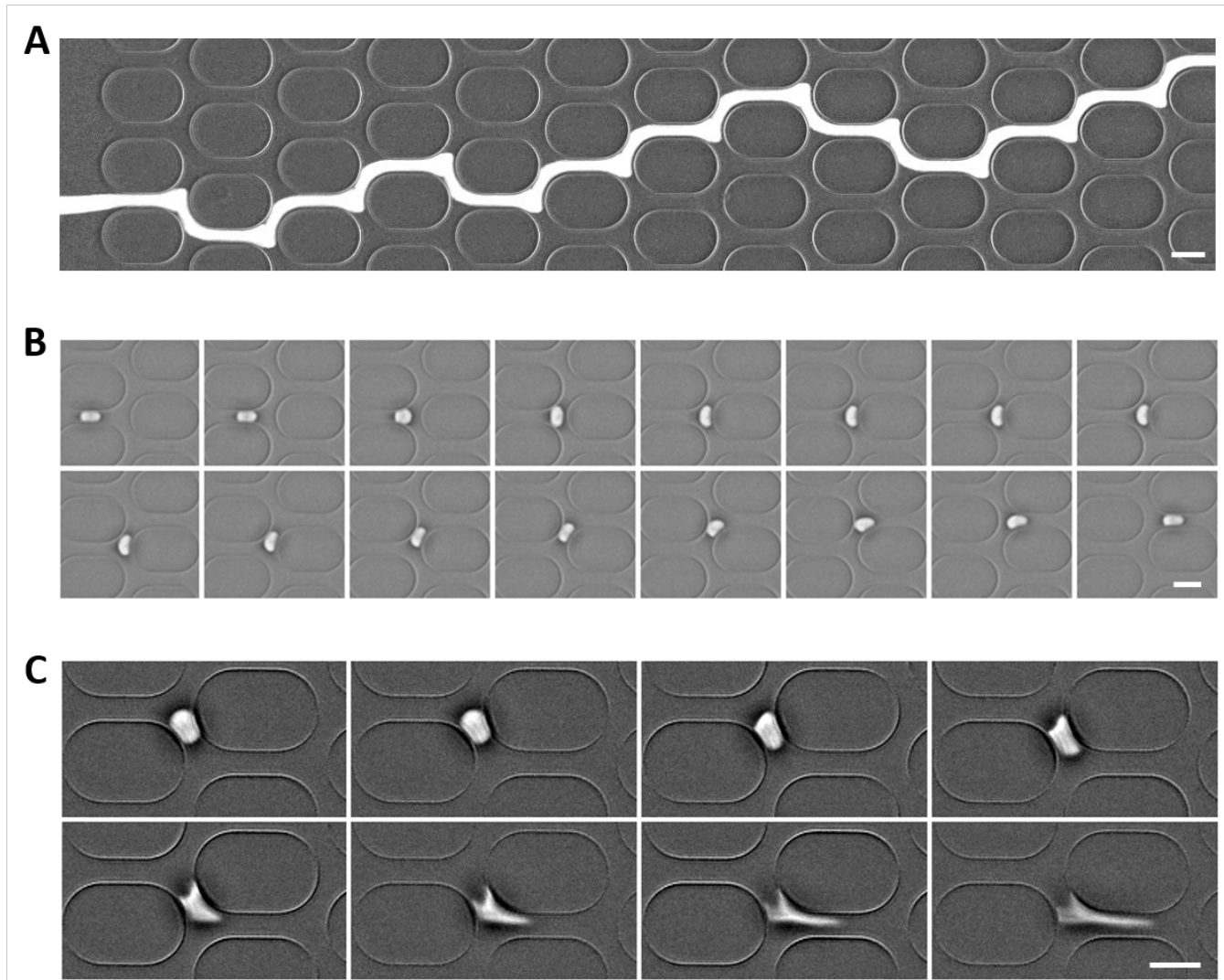


Fig. S4. Vesicles flowing through microchannel networks. The white pixels correspond to positions occupied by the vesicles, they were obtained by subtracting the network images to the movies and compiling pixels of maximum intensity, leading to a low contrast image of the networks. **A)** A vesicle larger than the channel width displays a random trajectory, $\Delta P = 5$ mbar. **B)** Timelapse of the vesicle in (A) passing through a mesh (0.04 sec between frames). Within the total duration of the mesh passage (0.6 sec), the vesicle hangs in the bifurcation for 0.2 sec. **C)** Timelapse of a rupturing vesicle unable to sustain the deformation by the channels (0.08 sec between frames), $\Delta P = 20$ mbar. Scale bars: 15 μm .

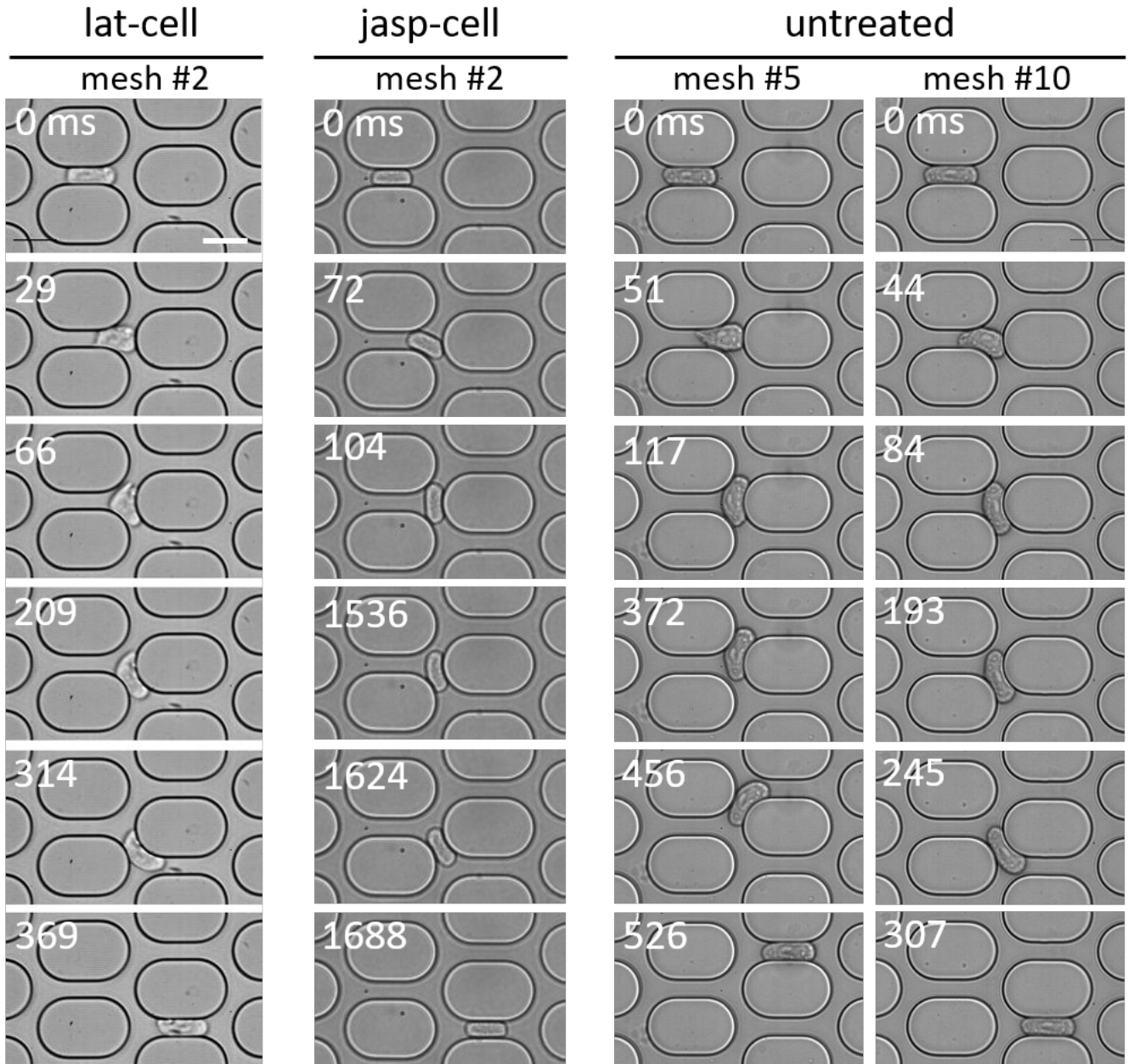


Fig. S5. Typical timelapses of cells during mesh passage. Lat-cells strongly deform much in the bifurcation while jasp-cells keep a rigid 'sausage' shape. Untreated cells display an intermediate behavior which evolves along the meshes: at mesh 5, the cell is slower than the lat-cell while at mesh 10 it passes within the same time. Scale bar: 20 μm .

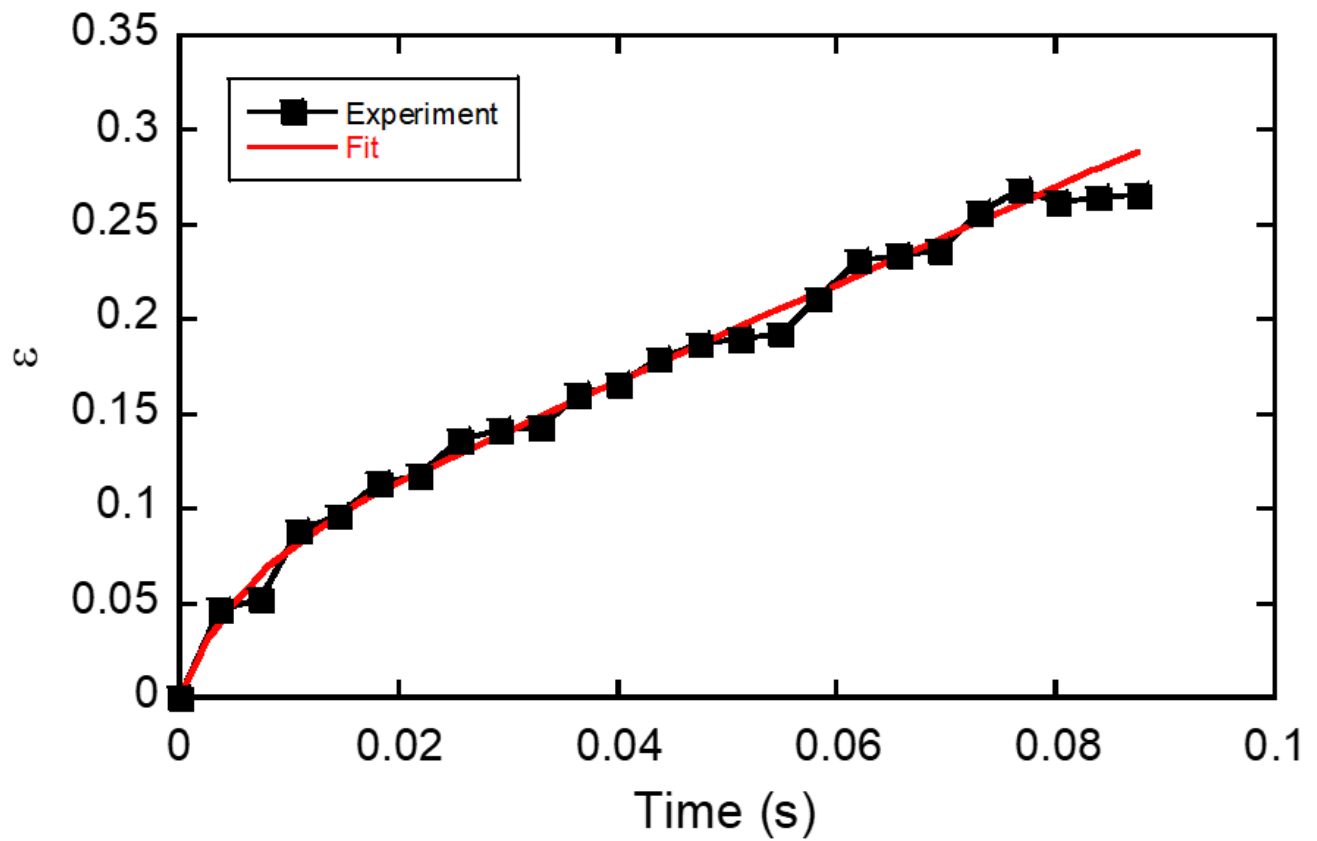


Fig. S6. Extraction of mechanical parameters for a lat-cell. Fitting the elongation ratio $\epsilon(t)$ of a 16.3- μm lat-cell entering a 9- μm channel network, by integration of Eq. 3 using simplified Eq. 4 ($\tau_0 = 0$), leads to $k_1 = 1830$ Pa, $\eta_1 = 14$ Pa.s, and $\eta_2 = 58$ Pa.s. $\Delta P = 40$ mbar.

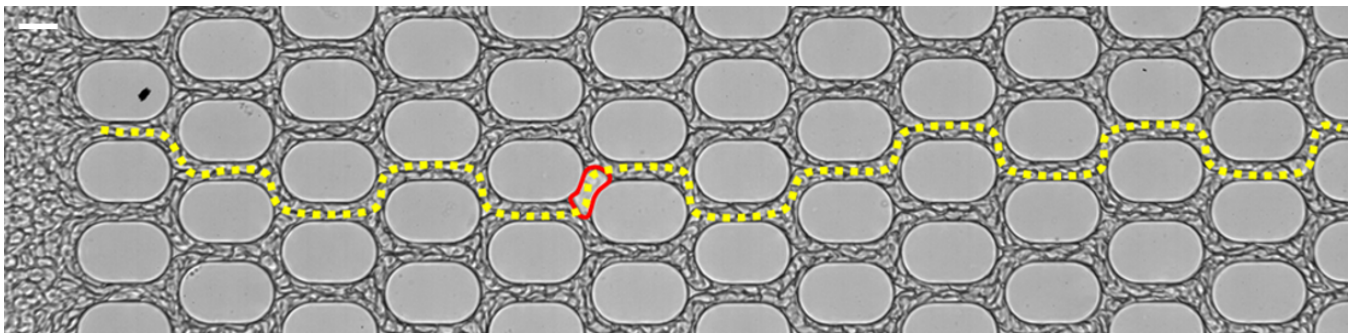


Fig. S7. Motion of a THP1 cell in a flowing suspension of concentrated red blood cells (RBCs) in the microchannel network. The cell displays a trajectory (in yellow) and a shape (in red) similar to those observed in absence of RBCs. Scale bar: 15 μm .

- 46 **Movie S1.** Passage of a 13.2- μm cell in the 8 first meshes of a 8.6- μm channel network. The movie corresponds
47 to Fig. 2.
- 48 **Movie S2.** A 16- μm cell alternately taking long (several sec) and short (less than a sec) times to pass through
49 successive meshes. It reaches the steady-state regime from mesh 6 where it then passes the meshes within
50 0.2 sec. The movie corresponds to black symbols in Fig. S3A.
- 51 **Movie S3.** Non-periodic trajectory of a GUV larger than the the microchannels, under a pressure drop of 5
52 mbar.
- 53 **Movie S4.** A 17- μm lat-cell immediately alternates between two parallel rows of channels in the network. It
54 strongly deforms when crashing on the pillar at exit of horizontal channel.
- 55 **Movie S5.** A 13- μm jasp-cell passes the meshes with random turns at exit of horizontal channels.
- 56 **Movie S6.** A 16- μm cell alternately takes long (1 or 2 sec) ans short (0.2-0.3 sec) times to pass through
57 successive meshes. It reaches the steady-state regime from mesh 10 where it then passes the meshes within
58 0.2 sec. The movie corresponds to blue symbols in Fig. S3A.
- 59 **Movie S7.** A very large lat-cell entering two channels and breaking into two parts.